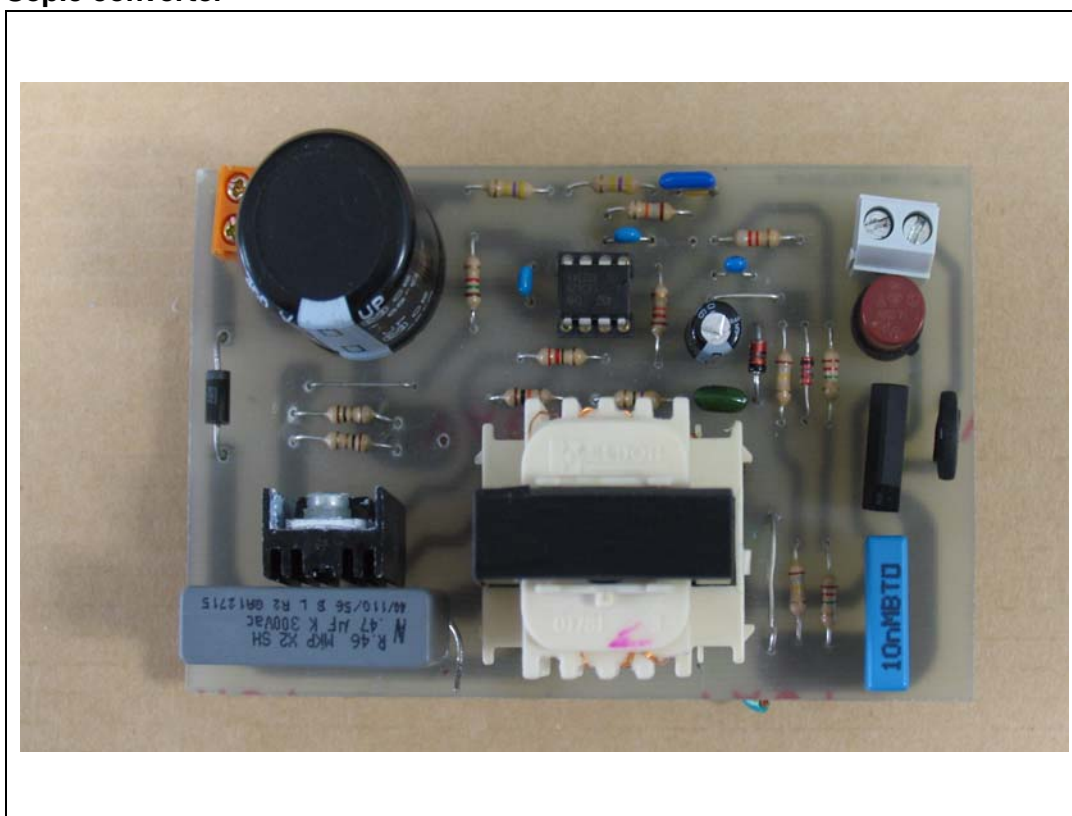


TM sepic converter in PFC pre-regulator

Introduction

For the PFC (power factor correction) converter, sepic topology can be used when an output voltage lower than the maximum input voltage is required. This is instead of boost topology, which is unsuitable because it must have an output voltage higher than the maximum input voltage. Sepic topology is advantageous because it allows the use of the ripple steering technique in order to reduce the switching frequency components of the input current without additional costs. This application note presents the basic equation of the sepic converter, in addition to design guidelines for a sepic PFC operating in transition mode and using the ripple steering technique. An application example with some tests results and waveforms is also provided in the document.

SePIC converter



Contents

1	Sepic topology for PFC converter	4
1.1	Operation of the sepic converter	4
1.2	Sepic converter as a PFC circuit operating in transition mode [1]	6
1.3	Coupled inductor sepic converter and ripple steering	10
1.4	Small signal model for a TM sepic converter	12
2	Practical design example of a sepic converter	13
2.1	Design specifications	13
2.2	MOSFET (M_1) selection	14
2.3	Diode D1 selection	14
2.4	Capacitor C1 selection	15
2.5	Output capacitor C2 selection	15
2.6	Transformer design	16
2.7	Selection of other components	17
3	Conclusion	18
3.1	References	18
4	Board description and bench evaluation results	18
4.1	Board description	18
4.2	Bench results	21
5	Revision history	24

List of figures

Figure 1.	Basic circuit of the sepic converter	5
Figure 2.	Sepic converter when the main switch is on.	5
Figure 3.	Sepic converter when the main switch is off.	6
Figure 4.	Inductor L1 and inductor L2 current waveform	6
Figure 5.	Switching frequency variation vs θ for two different input voltages.	9
Figure 6.	Input current in TM for sepic PFC	10
Figure 7.	Coupled inductor of a sepic converter	11
Figure 8.	Model of two coupled inductors	11
Figure 9.	Equivalent current source of the sepic converter	13
Figure 10.	Small signal model for the TM sepic converter.	13
Figure 11.	Output diode current averaged over the switching cycles	17
Figure 12.	Transformers with symmetrical structures	17
Figure 13.	Schematic of the sepic converter	20
Figure 14.	Efficiency chart	21
Figure 15.	Main waveform of the circuit.	22
Figure 16.	Current of the inductors over one line cycle: $V_{in} = 230 \text{ V}_{ACRMS}$, $P_{out} = 65 \text{ W}$	23
Figure 17.	Current of the inductors over switching cycles: $V_{in} = 230 \text{ V}_{ACRMS}$, $P_{out} = 65 \text{ W}$	23
Figure 18.	Current of the inductors over one line cycle: $V_{in} = 230 \text{ V}_{ACRMS}$, $P_{out} = 65 \text{ W}$	23
Figure 19.	Currents of the inductors over switching cycles: $V_{in} = 230 \text{ V}_{ACRMS}$, $P_{out} = 65 \text{ W}$	23
Figure 20.	Input current: 230 V_{ac} input, 65 W output	24
Figure 21.	Input current: 230 V_{ac} input, 32 W output	24

1 Sepic topology for PFC converter

The most widely used topology in PFC applications is boost topology. It has two main advantages:

1. The power switch is a low sided one, unlike buck and buck-boost topology where it is an high side one and needs a floating driving circuit.
2. The inductor is on the input side of the converter, limiting the slope of the input current.

The main disadvantage is that output voltage must always be higher than maximum input voltage, which may limit some applications and may be a problem when a lower output voltage is required.

Sepic topology has the above advantages and does not have the output voltage constraint. As in buck-boost topology, output voltage can be higher or lower than the input voltage. An additional advantage of sepic topology is that there are two inductors instead of one which can be wound in the same magnetic core. Using the proper turn ratio the input current ripple can be reduced theoretically to zero and the input filter for the conducted electro-magnetic interference strongly reduced (theoretically eliminated).

However, sepic topology, compared to boost topology, has the following disadvantages:

1. The MOSFET and the output diode break-down voltages are higher as they are the maximum reverse voltage when input and output voltages are summed (only output voltage for boost converter).
2. The current through the MOSFET is generally higher for the same output power.

1.1 Operation of the sepic converter

The basic schematic of the sepic converter is given in [Figure 1](#).

Assuming that the average voltage across each inductor during one switching cycle, in steady state operation, is zero, it can also be assumed that the average voltage over one switching cycle across capacitor C1 equals the input voltage of the converter.

If capacitor C1 is not too small, the voltage ripple across C1 (V_{C1}) is negligible, and it can be assumed that over one switching cycle, this voltage stays constant and equals the input voltage (V_{IN}). This hypothesis ($V_{C1} = V_{IN}$) is the starting point for sepic converter analysis.

When the main switch (M_1) of the sepic converter is on, input voltage is applied to inductor L₂ (see [Figure 2](#)). In steady state condition, the same voltage is applied to inductor L1 which is in parallel with capacitor C1. The reverse voltage applied on diode D₁ is the sum of the input and output voltage ($V_{IN} + V_{OUT}$) and the current through M1 is the sum of the currents through inductor L1 and inductor L2 ($I_{L1} + I_{L2}$).

Across inductor L1 and inductor L2 we have the same voltages and the currents through them rise linearly with slopes inversely proportional to their inductances values.

When M1 is switched off ([Figure 3](#)), diode D1 starts to conduct and the energy previously stored in inductor L1 and inductor L2 is released to restore the energy used up by capacitor C1 and capacitor C₂ when M1 was on. This energy also supplies the load. *The voltage across the MOSFET is the sum of the voltage across capacitor C1, which is equal to the sum of the input and the output voltage.*

The current through diode D1 is the sum of the currents running through inductor L1 and inductor L2. The voltage across both inductors is equal to V_{OUT} , and the current slope is negative and inversely proportional to inductor L1 and inductor L2 respectively.

Figure 4 shows the theoretical waveforms of the inductors' currents. Equation 1 and Equation 2 give the waveform expressions during turn-on (T_{ON}), whilst Equation 3 and Equation 4 give the waveform expressions during turn-off (T_{OFF}).

Equation 1

$$I_{L1}(t) = I_{L10} + \frac{V_{IN}}{L_1} \cdot t$$

Equation 2

$$I_{L2}(t) = I_{L20} + \frac{V_{IN}}{L_2} \cdot t$$

Equation 3

$$I_{L1}(t) = I_{L10} + \frac{V_{IN}}{L_1} \cdot T_{ON} - \frac{V_{out}}{L_1} \cdot t$$

Equation 4

$$I_{L2}(t) = I_{L20} + \frac{V_{IN}}{L_1} \cdot T_{ON} - \frac{V_{out}}{L_2} \cdot t$$

Figure 1. Basic circuit of the sepic converter

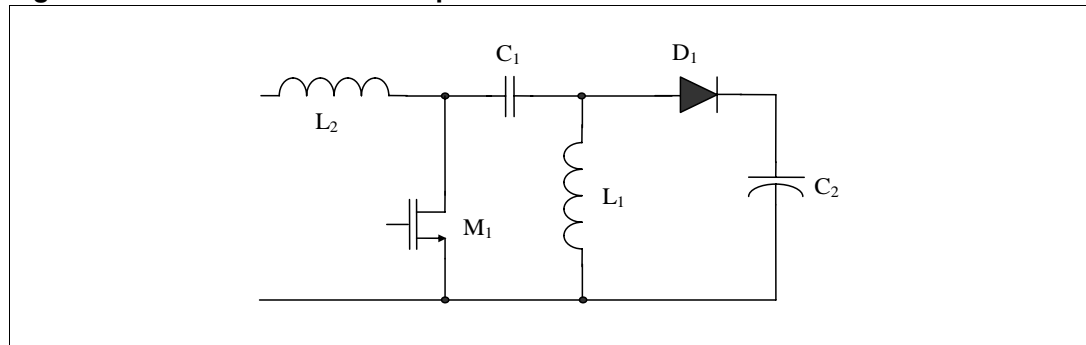


Figure 2. Sepic converter when the main switch is on

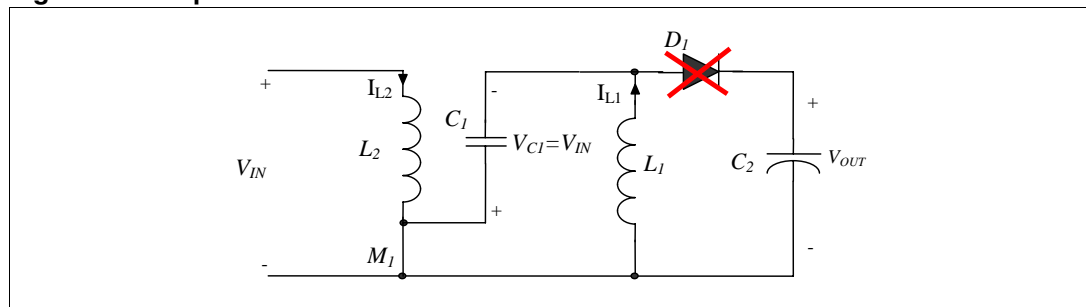


Figure 3. Sepic converter when the main switch is off

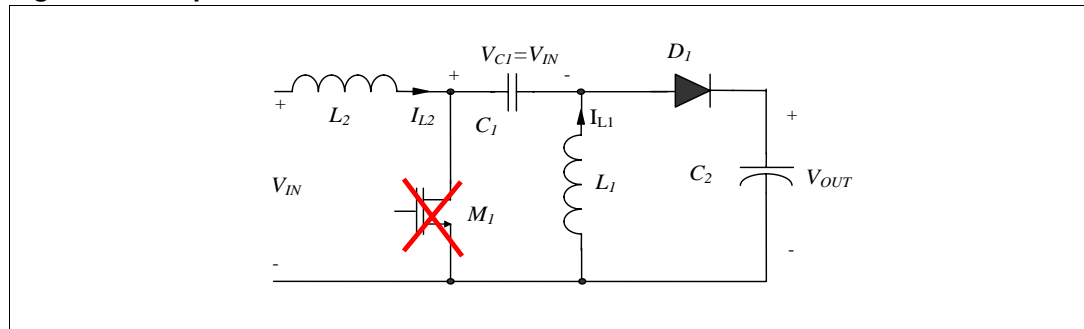
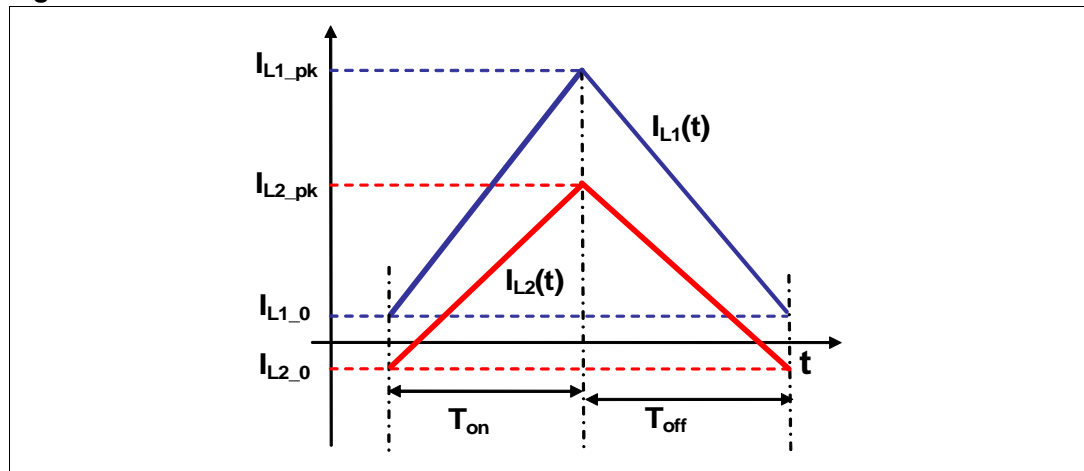


Figure 4. Inductor L1 and inductor L2 current waveform



1.2 Sepic converter as a PFC circuit operating in transition mode [1.]

In PFC applications, input voltage is the rectified main and it changes according to the equation:

Equation 5

$$V_{IN}(\vartheta) = \sqrt{2} \cdot V_{ac} \cdot |\sin(\vartheta)|$$

where ϑ is $2\pi f_L t$, f_L is the line frequency, and V_{ac} is the rms value of the line voltage.

As switching frequency is in the range of some tenth of kHz, and thus much higher than the line frequency, we can assume ϑ is constant over each switching cycle.

The L6562 (see [2]) is a current mode controller dedicated to PFC applications. It is used in this instance. It senses the MOSFET current and the input voltage of the converter (rectified main), through a sense resistor and a resistor divider respectively. Cycle by cycle the MOSFET is switched-off as the sensed current reaches a limit set by the controller. This limit is proportional to the sensed input voltage so, the MOSFET peak current ($I_{PK}(t)$) follows a sinusoidal reference:

Equation 6

$$I_{PK}(t) = I_{PK} \cdot |\sin(\vartheta)|$$

Taking into account that input voltage is now the rectified main, [Equation 1](#) and [Equation 2](#) can be rewritten as follows:

Equation 7

$$I_{L1}(t, \vartheta) = I_{L10} + \frac{V_{IN}(\vartheta)}{L_1} \cdot t, \quad I_{L2}(t, \vartheta) = I_{L20} + \frac{V_{IN}(\vartheta)}{L_2} \cdot t$$

Due to transition mode operation, the MOSFET is switched on as soon as the diode current falls to zero. This means that:

Equation 8

$$I_{L10} - I_{L20} = 0$$

From and [Equation 8](#), the MOSFET peak current equation may be derived:

Equation 9

$$I_{PK}(\vartheta) = \left(\frac{1}{L_1} + \frac{1}{L_2} \right) \cdot t_{ON}(\vartheta) \cdot \sqrt{2} \cdot V_{ac} \cdot \sin(\vartheta)$$

Combining [Equation 9](#) and [Equation 6](#) an expression for T_{ON} may be obtained:

Equation 10

$$t_{ON}(\vartheta) = \frac{I_{PK} \cdot \sin(\vartheta)}{\left(\frac{1}{L_1} + \frac{1}{L_2} \right) \cdot \sqrt{2} \cdot V_{ac} \cdot \sin(\vartheta)} = \frac{L_e \cdot I_{PK}}{\sqrt{2} \cdot V_{ac}} = T_{ON}$$

where L_e is the parallel between inductor L_1 and inductor L_2 . [Equation 10](#) indicates that, as in TM (Transition Mode) boost converter T_{ON} is independent from ϑ .

The expression for T_{OFF} is obtained in a similar way to above:

Equation 11

$$T_{OFF}(\vartheta) = \frac{T_{ON} \cdot \sqrt{2} \cdot V_{ac} \cdot \sin(\vartheta)}{V_O}$$

where V_O is the output voltage. The off time is dependent on θ , as in TM boost converter.

Once T_{ON} and T_{OFF} are known, switching frequency (f_{SW}) may be easily calculated as it is a function of ϑ :

Equation 12

$$f_{SW}(\vartheta) = \frac{1}{T_{ON} + T_{OFF}(\vartheta)} = \frac{1}{T_{ON} \cdot \left(1 + \frac{\sqrt{2} \cdot V_{ac} \cdot |\sin(\vartheta)|}{V_O} \right)}$$

[Figure 5](#) shows the switching frequency versus θ for two different input voltages. To calculate input current averaged over one switching cycle, [Equation 13](#), the charge balance on capacitor C_1 , is used:

Equation 13

$$\left(I_{L10}(\vartheta) + \frac{1}{2} \cdot \frac{V_{IN}(\vartheta)}{L_1} \cdot T_{ON} \right) \cdot T_{ON} = \left(I_{L20}(\vartheta) + \frac{1}{2} \cdot \frac{V_{IN}(\vartheta)}{L_2} \cdot T_{ON} \right) \cdot T_{OFF}(\vartheta) = Q(\vartheta)$$

where $Q(\vartheta)$ indicates the quantity of electrical charge that flows through capacitor C1, cycle by cycle.

Combining [Equation 8](#) and [Equation 13](#), $I_{L2(0)}(\vartheta)$ may be calculated as follows:

Equation 14

$$I_{L20}(\vartheta) = \frac{f_{SW}(\vartheta) \cdot V_{IN}(\vartheta) \cdot T_{ON}}{2} \cdot \left[\frac{T_{ON}}{L_1} - \frac{T_{OFF}(\vartheta)}{L_2} \right]$$

Using equation 14, I_{L2avg} may then be calculated using [Equation 15](#):

Equation 15

$$I_{L2avg}(\vartheta) = \frac{1}{2} \cdot \frac{V_{IN}(\vartheta)}{L_2} \cdot T_{ON} + I_{L20}(\vartheta) = \frac{1}{2} \cdot I_{PK} \cdot \frac{|\sin(\vartheta)|}{1 + \frac{\sqrt{2} \cdot V_{AC}}{V_O} |\sin(\vartheta)|}$$

[Equation 15](#) shows that the input current is not exactly sinusoidal. A certain amount of distortion is related to the quantity K_V , which is defined as follows:

$$K_V = \frac{\sqrt{2} \times V_{AC}}{V_O}$$

[Figure 6](#) shows the input currents (before the bridge diodes) for different values of V_{AC} . The first input current, $I_0(\theta)$, is calculated for $K_V=0$. It is used only as a reference, because it is completely sinusoidal. In this instance, V_O is considered to be 200 V. The second input current, $I_1(\theta)$, is at $V_{AC} = 265$ V and the third, $I_2(\theta)$, is the input current at $V_{AC} = 175$ V. All currents are normalized in accordance with their respective RMS values. In figure 6, the distortion of the current with respect to a perfect sinusoid is obvious. Even though such distortion is present, quite high values for the power factor are obtained. The voltage across capacitor C1 averaged over one switching cycle is the same as the input voltage. There is an additional voltage ripple due to the currents of the inductors across capacitor C1. Its amplitude ($\Delta V_{C1}(\vartheta)$) is calculated below:

Equation 16

$$\Delta V_{C1}(\vartheta) = \frac{V_{IN}(\vartheta) \cdot T_{ON}^2}{C_1 \cdot L_e} \cdot \frac{T_{OFF}(\vartheta)}{T_{ON} + T_{OFF}(\vartheta)}$$

Substituting the values of T_{ON} (Equation 10), T_{OFF} (Equation 11), and $V_{IN}(\theta)$ (Equation 5), $\Delta V_{C1}(\vartheta)$ may be expressed as follows:

Equation 17

$$\Delta V_{C1}(\vartheta) = \frac{L_e}{C1} \cdot \frac{I_{PK}^2}{2} \cdot \frac{|\sin(\vartheta)|^2}{(V_O + \sqrt{2} \cdot V_{ac} \cdot |\sin(\vartheta)|)}$$

It is useful to rewrite some quantities calculated earlier, in terms of converter output power, RMS input voltage (V_{AC}), and expected efficiency (η), because these quantities are generally known at the beginning of a design. Input power may be expressed as follows:

Equation 18

$$P_{in} = f_L \cdot \int_0^{\frac{1}{f_L}} \left[\frac{I_{PK}}{2} \cdot \frac{\sin(2\pi f_L \cdot t)}{1 + k_V \cdot |\sin(2\pi f_L \cdot t)|} \cdot \sqrt{2} \cdot V_{ac} \cdot \sin(2\pi f_L \cdot t) \right] \cdot dt$$

($F(k_V)$) may be calculated as follows:

Equation 19

$$F(k_V) = f_L \cdot \int_0^{\frac{1}{f_L}} \left[\frac{\sin^2(2\pi f_L \cdot t)}{1 + k_V \cdot |\sin(2\pi f_L \cdot t)|} \right] \cdot dt$$

I_{PK} may be expressed as follows:

Equation 20

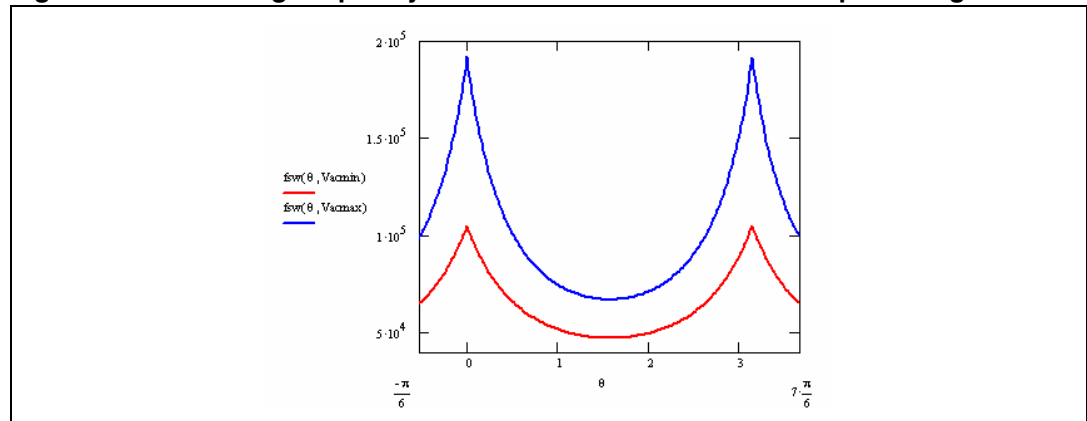
$$I_{PK} = \frac{2 \cdot P_O}{\eta \cdot \sqrt{2} \cdot V_{ac} \cdot F(k_V)}$$

The switching frequency can be expressed as:

Equation 21

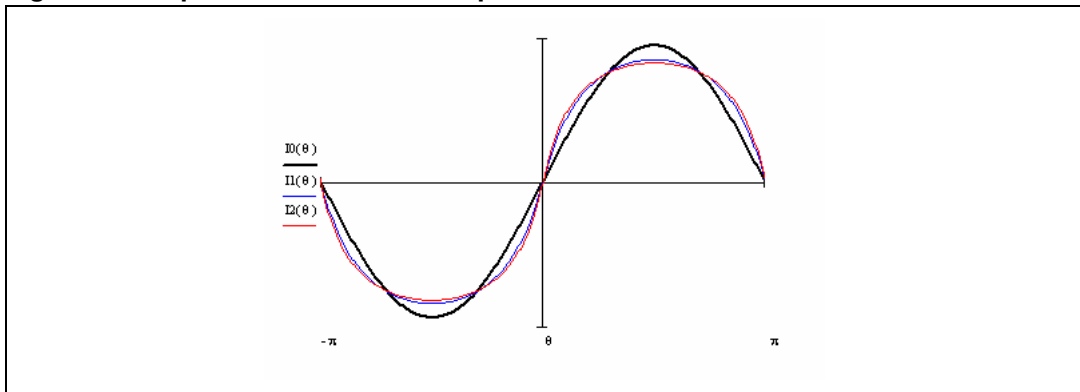
$$f_{sw}(\vartheta) = \frac{\eta \cdot V_{ac}^2 \cdot F(k_V)}{P_O \cdot L_e \cdot (1 + k_V \cdot |\sin(\vartheta)|)}$$

Figure 5. Switching frequency variation vs θ for two different input voltages



1. Where $V_{acmin} = 175$ V, $V_{acmax} = 265$ V, $L_e = 1$ mH, $h = 0.9$, and $P_O = 65$ W.

Figure 6. Input current in TM for sepic PFC



1.3 Coupled inductor sepic converter and ripple steering

If the two inductors are wound in the same magnetic core, it is possible to reuse the equations used in [Section 1.2](#). Moreover, the current ripple in the input inductor L_2 can theoretically be reduced to zero, simply by selecting the correct turn ratio. A model of two coupled inductors is shown in [Figure 8](#). L_{lk1} and L_{lk2} are the leakage inductances, L_M is the magnetizing inductance and n is the turn ratio.

The equations that describe the coupled inductor model of [Figure 8](#) are given below.

Equation 22

$$\begin{cases} v_1(t) = L_{L1} \cdot \frac{di_1(t)}{dt} + L_M \cdot \frac{di_M(t)}{dt} \\ v_2(t) = L_{L2} \cdot \frac{di_2(t)}{dt} + n \cdot L_M \cdot \frac{di_M(t)}{dt} \\ \frac{di_M}{dt} = \frac{di_1}{dt} + n \cdot \frac{di_2(t)}{dt} \end{cases}$$

In the first two sub equations of [Equation 22](#), the derivate of the magnetizing current (i_M) can be substituted with the value given in sub-equation 3.

Considering that the same voltage is applied to both inductors we have:

Equation 23

$$\begin{cases} v_1(t) = L_{EQ1} \cdot \frac{di_1(t)}{dt} \\ v_2(t) = L_{EQ2} \cdot \frac{di_2(t)}{dt} \end{cases}$$

Equation 24

$$\begin{cases} L_{EQ1} = \frac{L_{L1} \cdot L_{L2} + L_M \cdot L_{L2} + n^2 \cdot L_M \cdot L_{L1}}{L_{L2} + n \cdot (n - 1) \cdot L_M} \\ L_{EQ2} = \frac{L_{L1} \cdot L_{L2} + L_M \cdot L_{L2} + n^2 \cdot L_M \cdot L_{L1}}{L_{L1} - (n - 1) \cdot L_m} \end{cases}$$

The main conclusion of [Equation 23](#) and [Equation 24](#), is that the same equations can be used for coupled and uncoupled inductors. If no current flows on the secondary side, voltage V_2 is the same as voltage V_2^1 (see [Figure 8](#)) and may be written as follows:

Equation 25

$$V_2 = V_2^1 = n \cdot V_1^1 = n \cdot \frac{L_M}{L_M + L_{LK1}} \cdot V_1$$

As the same voltage is applied, simultaneously, to both inductors in a sepic converter, [Equation 25](#) may be simplified below as:

Equation 26

$$n \cdot \frac{L_M}{L_M + L_{LK1}} = 1$$

When the above ‘ripple steering’ condition is verified theoretically, the voltage across L_{LK2} is zero and no current flows on the secondary side. In the actual circuit only the high frequency components of the inductor L2 current are attenuated. Once [Equation 26](#) is verified, [Equation 24](#) may be simplified as:

Equation 27

$$\begin{cases} L_{EQ1} = L_M + L_{LK1} \\ L_{EQ2} = \infty \end{cases}$$

Therefore, for a sepic converter with coupled inductors, infinite inductance at the input may be seen theoretically once [Equation 26](#) is satisfied. In the actual circuit, due to imperfect matching with [Equation 26](#) and due to the fact that the voltages applied to the two inductors are not exactly the same (because of the voltage ripple on capacitor C1), a large input inductance may be seen at the converter input. This input inductance helps the line filter in eliminating the switching frequency component of the input current.

Figure 7. Coupled inductor of a sepic converter

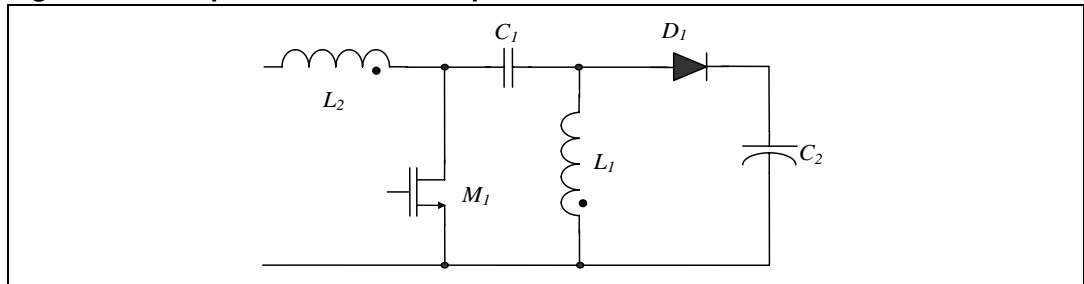
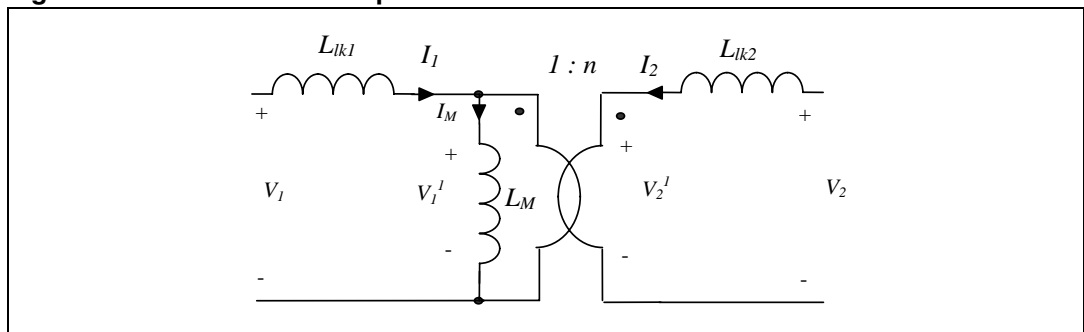


Figure 8. Model of two coupled inductors



1.4 Small signal model for a TM sepic converter

It is possible to model the output stage of the sepic converter as a current source. The sourced current is a function of the input voltage RMS value, the output voltage, and the MOSFET peak current. To obtain the necessary function, the output diode current may first be averaged over each switching cycle, to give the following equation:

Equation 28

$$I_{D1}(\vartheta) = \frac{k_{vmin}}{2} \cdot \frac{I_{PK} \cdot (\sin(\vartheta))^2}{1 + k_v \cdot |\sin(\vartheta)|}$$

Assuming that the control loop reaction must be very slow to remain constant over a single line cycle, then to ensure high PFC, [Equation 28](#) may be averaged with respect to θ as follows:

Equation 29

$$I_{D1avg}(V_{ACRMS}, V_O, I_{PK}) = \frac{1}{2} \cdot \frac{\sqrt{2} \cdot V_{ACRMS}}{V_O} \cdot I_{PK} \cdot F\left(\frac{\sqrt{2} \cdot V_{ACRMS}}{V_O}\right)$$

For small variations of its argument, the I_{D1AVG} function may be approximated with a linear function, and the output stage of the sepic converter may be represented by the circuit in [Figure 10](#). Bearing in mind that $F(K_v)$ was defined in [Equation 19](#), expressions for g_2 (see [Figure 10](#)), e_2 (see [Figure 10](#)) and r_2 (see [Figure 10](#)) are given below:

Equation 30

$$g_2 = \frac{\partial I_{D1AVG}}{\partial I_{ACRMS}}$$

$$e_2 = \frac{\partial I_{D1AVG}}{\partial I_{PK}} = \frac{1}{2} \cdot K_v \cdot F(K_v)$$

$$r_2 = -\left[\frac{\partial I_{D1AVG}}{\partial V_O}\right]^{-1} = \left[\frac{I_{PK}}{2 \cdot V_O} \cdot K_v \cdot \left(F(K_v) + K_v \cdot \frac{\partial F(K_v)}{\partial K_v}\right)\right]^{-1}$$

It should be remembered that K_v was defined as:

$$K_v = \frac{\sqrt{2} \times V_{AC}}{V_O}$$

Also, note that g_2 is not calculated here because is not used in the control Loop design. Then, using [Figure 10](#) and the sub-equations of [Equation 30](#), it is possible to deduce the small signal transfer function (control to output) $G(s) = V_{COMP}(s)/V_O(s)$.

Equation 31

$$G(s) = \frac{\partial \hat{V}_O}{\partial \hat{V}_{COMP}} = \frac{G_O}{1 + \frac{s}{\omega_p}}$$

where the gain (G_O) and the pole frequency (ω_p) are defined below:

Equation 32

$$G_O = K_P \cdot K_M \cdot e_2 \cdot \frac{\sqrt{2} \cdot V_{ACrms}}{R_{SENSE}} \cdot \frac{r_2 \cdot R_O}{r_2 + R_O}, \quad \omega_p = \frac{r_2 - R_O}{C_2 \cdot r_2 \cdot R_O}$$

where (R_O) is the assumed resistive load.

Figure 9. Equivalent current source of the sepic converter

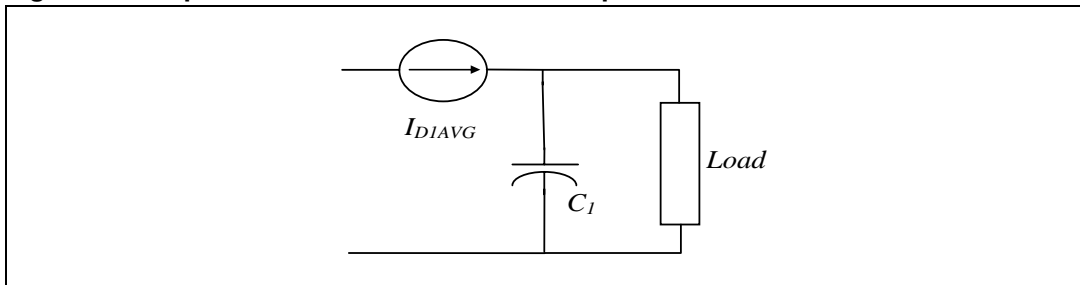
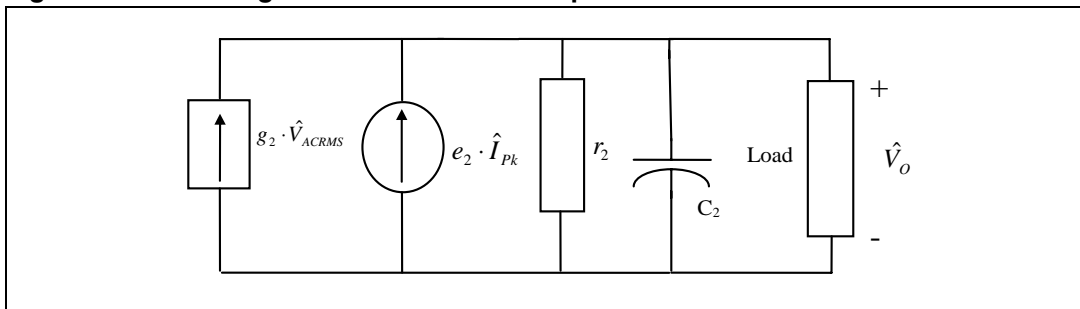


Figure 10. Small signal model for the TM sepic converter



2 Practical design example of a sepic converter

A practical example of a sepic converter is described below.

2.1 Design specifications

For the input data, the design specifications are needed.

Table 1. Design specification

Quantity	Value
Mains voltage range: $V_{INMIN (RMS)} - V_{INMAX (RMS)}$	175 V_{ACRMS} - 265 V_{ACRMS}
Regulated DC output voltage	200 V
Rated Output Power: P_O	65 W
Minimum switching frequency: f_{swmin}	45 kHz
Maximum over-voltage admitted: ΔV_{OVP}	40 V
Maximum output voltage ripple ΔV_O	20 V
Expected efficiency: η	90 %
Maximum mains RMS current	$I_{INRMSMAX} = \frac{P_O}{\eta \cdot V_{ACMIN}} = 420mA$

Table 1. Design specification (continued)

Quantity	Value
Rated output current: I_O	$I_O = \frac{P_O}{V_O} = 325\text{mA}$
Output equivalent resistor	$I_O = \frac{V_O^2}{P_O} = 615\Omega$

The complete schematic of the circuit is given in [Figure 13](#).

2.2 MOSFET (M₁) selection

The MOSFET peak current value (I_{PK}) is calculated using [Equation 18](#). Substituting the quantities given in the electrical specifications, the MOSFET peak current value is $I_{PK} = 2.36\text{ A}$. The RMS value of the current flowing through the MOSFET may be calculated using [Equation 33](#):

Equation 33

$$I_{M1RMS} = I_{PK} \sqrt{\frac{F(K_{Vmin})}{3}} = 0.678\text{A}$$

where:

Equation 34

$$K_{Vmin} = \frac{\sqrt{2} \cdot V_{ACMIN(RMS)}}{V_O}$$

Under the worst case scenario, the MOSFET and the output diode have to sustain a voltage that is the sum of the maximum peak input voltage and the maximum output voltage. Considering the electrical specifications above and a safety margin of 10%, the minimum breakdown voltage ($B_{DVSSMin}$) for M1 is:

Equation 35

$$B_{DVSSMin} = (\sqrt{2} \cdot V_{ACmax} + V_O + \Delta V_{OVP}) \cdot 1.1 = (375\text{V} + 200\text{V} + 40\text{V}) \cdot 1.1 = 677\text{V}$$

To avoid large heat sink, the RMS value of the through current suggests using a MOSFET with an R_{DSON} not greater than $1.5\ \Omega$. The selected MOSFET, the STP9NK70, has a maximum R_{DSON} of $1.2\ \Omega$ at $25\ ^\circ\text{C}$ and a breakdown voltage of 700 V .

2.3 Diode D1 selection

The average value of the diode D1 current is the output current. The RMS value of the current flowing through diode D1 can be calculated using the following formula:

Equation 36

$$I_{D1RMS} = I_{PK} \sqrt{\frac{1}{3} \cdot \frac{1}{\pi} \cdot \int_0^\pi \frac{K_{Vmin} \cdot |\sin(\vartheta)|^3}{0.1 + K_{Vmin} \cdot |\sin(\vartheta)|^3} \cdot d\vartheta} = 0.687\text{A}$$

The minimum breakdown voltage of diode D1 is the same as for the MOSFET. The selected diode D1, STTH208, has a breakdown voltage of 800 V. When it is forward biased, the voltage drop, (V_d) is 1.05 V and the dynamic resistance (r_d) is 100 m Ω . The power dissipation on D1 may easily be calculated as follows:

Equation 37

$$P_{D1Loss} = V_d \cdot I_O + r_d \cdot I_{D1RMS}^2 = 0.388W$$

2.4 Capacitor C1 selection

The equivalent inductance L_e must be calculated, using [Equation 38](#) and knowing the minimum switching frequency, the output power, and the efficiency from previous electrical specifications:

Equation 38

$$L_e = \frac{\eta \cdot V_{ACMIN(RMS)}^2 \cdot F(k_{vmin})}{P_O \cdot f_{swmin} \cdot (1 + k_{vmin})} = 1041mH \cong 1mH$$

The value of capacitor C1 may be selected by imposing the maximum voltage ripple across it. Considering a maximum voltage ripple of 15 V

$\Delta V_{C1MAX} = 15V$ and using [Equation 21](#), the following formula may be calculated:

Equation 39

$$C_1 = \frac{L_e}{\Delta V_{C1MAX}} \cdot \frac{I_{PK}^2}{2} \cdot \frac{1}{(V_O + \sqrt{2} \cdot V_{acmin})} = 416nF$$

A 470 nF capacitor was selected.

It is important to note that the voltage ripple on capacitor C1 will affect the ripple steering effect.

The difference between the voltages across the two inductors, either when the MOSFET is on or off, is the difference between the voltage on capacitor C1 and the input voltage, which effectively is the switching frequency voltage ripple, across capacitor C1.

Because of this ripple, the two inductors do not have exactly the same voltage. Even when [Equation 26](#) is perfectly satisfied, the current ripple on the input inductor L2 is not zero.

2.5 Output capacitor C2 selection

The output diode current, averaged over each switching cycle, is given in [Equation 29](#). The graph of this waveform is shown in [Figure 11](#). The quantity of electrical charge that goes into capacitor C2 is the same as the integral of the diode current:

Equation 40

$$C_2 \cdot V_O(\vartheta) = X(\vartheta) = \int_0^{\vartheta} I_{D1}(\alpha) \cdot d\alpha$$

Under steady state conditions, the output voltage is maximum and minimum at the two points where $I_{D1}(\theta)$ equals the output current I_O . Letting these angles be θ_1 and θ_2 , the minimum output capacitor value that guarantees an output voltage ripple lower than the specified ΔV_O is:

Equation 41

$$C_2 = \frac{|X(\vartheta_1) - X(\vartheta_2)|}{2 \cdot \pi \cdot f_L \cdot \Delta V_O}$$

2.6 Transformer design

The selected magnetic core is an ETD29 made with N67 material. The effective area (A_e) of this core is 0.76 cm². Once the core is selected, the minimum turn number, which prevents the transformer from saturation or overheating, may be calculated using the formula:

Equation 42

$$N_{2min} = \frac{V_{in} \cdot T_{ON}}{A_e \cdot \Delta B}$$

The maximum magnetic swing (ΔB) selected is 0.25 T. In the current design the number of turns for the inductor L2 is 125.

If the ripple steering condition is satisfied, [Equation 43](#) (below) may be calculated using [Equation 24](#):

Equation 43

$$L_e = \left(\frac{1}{L_{EQ1}} + \frac{1}{L_{EQ2}} \right)^{-1} = L_{LK1} + L_M = L_{OP1}$$

It may be used to select the proper air gap, where L_{OP1} is the inductance measured at the primary side with the secondary side open. Selecting the correct turn ratio to meet the ripple steering condition for an actual transformer (rather than a theoretical one) is not easy, as the internal parameters of the transformer (L_M and L_{LK1}) are unknown. [Equation 44](#) is equivalent to [Equation 26](#) but is based on measurable quantities. L_{SH1} and L_{OP1} are the primary inductances, measured when the secondary side is shorted and when the secondary side is open, respectively.

Equation 44

$$n = \sqrt{\frac{L_{OP1}}{L_{OP1} - L_{SH1}}}$$

[Equation 44](#) is obtained using the hypothesis expressed in [Equation 45](#):

Equation 45

$$L_{LK1} = \frac{1}{n^2} \cdot L_{LK2}$$

[Equation 45](#) is generally true if the transformer has a 'symmetrical structure'. [Figure 12](#) shows two examples of transformers with a symmetrical structure. A slotted transformer ([Figure 12 b](#)) is used in the board for the current document. The selected turn ratio (n) is 1.28, which gives a value of 98 turns for the inductor L1.

2.7 Selection of other components

Selection of the other components of the circuit may be made using the guidelines for a boost converter which are given in [2]. Capacitor C1 must be considered in parallel with the input capacitor, which means that a small capacitor of 10 nF is adequate for the current design.

For the control loop design the procedure used for a boost converter in [4] may be followed. The small signal model developed in this document must be considered.

The charge pump which supplies the IC, while respecting the calculated steady state values, needs to be a little over-sized. During start-up, capacitor C2 is not pre-charged by the inrush current as in a boost converter, and therefore, the charge pump provides less current. In order not to have too big a charge pump, the capacitor on the V_{CC} pin of the L6562 has to be increased during start up phase to supply the IC, even if the charge pump is not able to provide enough current.

Figure 11. Output diode current averaged over the switching cycles

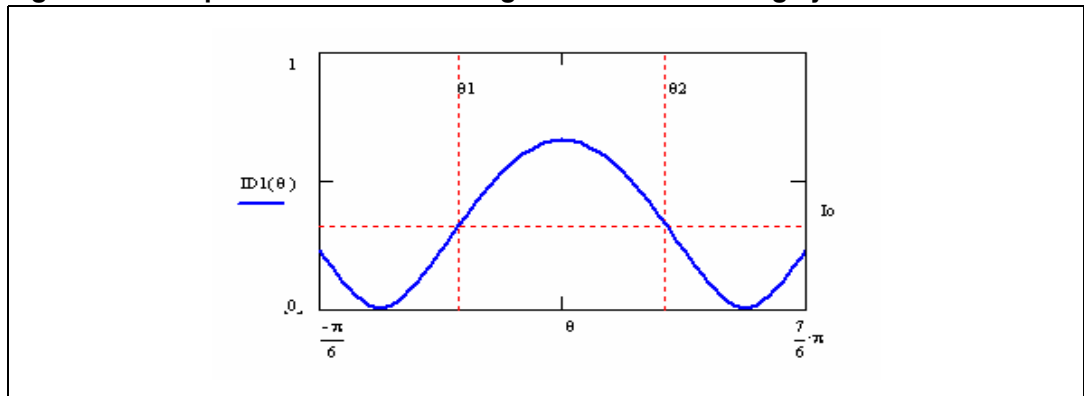
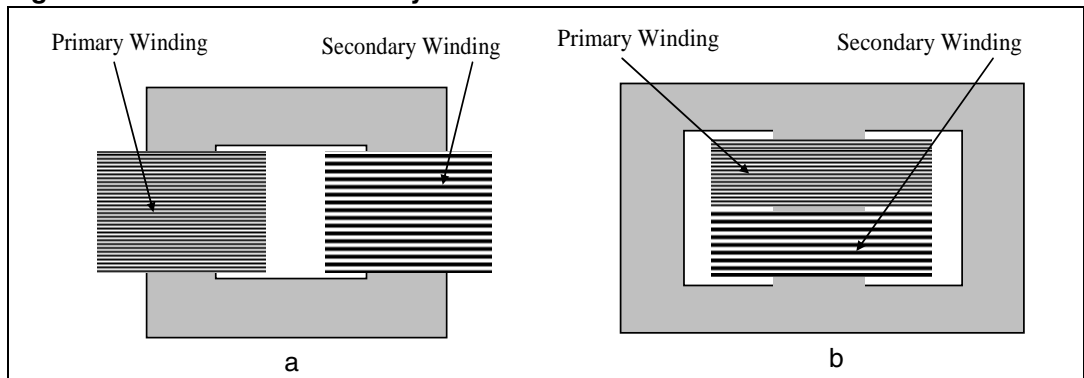


Figure 12. Transformers with symmetrical structures



3 Conclusion

This document presented the sepic converter operating in transition mode for power factor correction applications. The ripple steering technique was also presented. The basic theory behind the sepic converter and the ripple steering technique was discussed and design equations were outlined. An example of a design was proposed.

3.1 References

1. Analysis and design of SEPIC converter in boundary conduction mode for universal-line power factor correction applications. From Power Electronics Specialists Conference, 2001. PESC. 2001 IEEE 32nd Annual.
2. L6561, enhanced transition mode power factor corrector (AN966).
3. Minimize filtering with ripple steering. Published in Analog Zone.
4. Control loop modeling of L6561-based TM PFC (AN1089)
5. Transition-mode PFC controller (L6562 datasheet)

4 Board description and bench evaluation results

4.1 Board description

This section gives the bill of material and the schematic of the board according to the electrical specifications given in [Section 2](#).

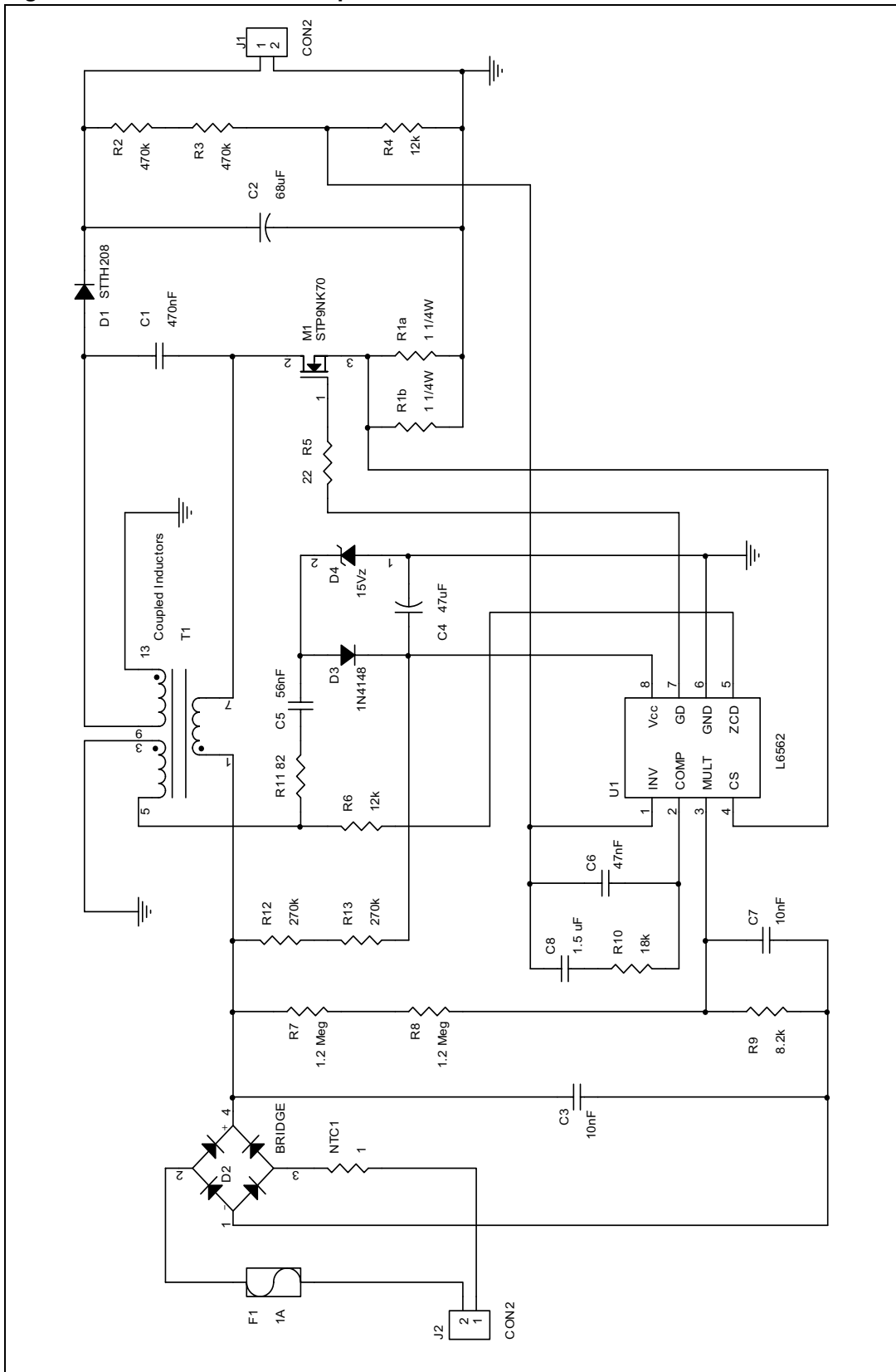
Table 2. Bill of material

Part	Value	Description
C1	470 nF	630 V capacitor
C2	68 μ F	250 V electrolytic capacitor
C3	10 nF	X2 type capacitor
C4	47 μ F	25V electrolytic capacitor
C5	56 nF	100 V capacitor
C6	47 nF	Small signal capacitor
C7	10 nF	Small signal capacitor
C8	1.5 μ F	Small signal capacitor
D1	STTH208	STMicroelectronics high voltage ultrafast rectifier
D2	BRIDGE	600 V, 1 A standard bridge diode
D3	1N4148	Standard diode
D4	15 Vz	15 V zener diode
F1	1 A	1 A fuse

Table 2. Bill of material (continued)

Part	Value	Description
NTC1	1	1 Ohm NTC
Q1	STP9NK70	STMicroelectronics N-Channel 700 V supermesh tm power MOSFET
R1a, R1b	1 Ohm	1 % precision resistor
R2, R3	470 Kohm	1 % precision resistor
R4	12 Kohm	1 % precision resistor
R5	22 Ohm	Resistor
R6	12 Kohm	Resistor
R7, R8	1.2 Megaohm	Resistor
R9	8.2 Kohm	Resistor
R10	18 Kohm	Resistor
R11	82 Ohm	Resistor
R13,R12	270 Kohm	Resistor
T1	Coupled inductors	
U1	L6562	Transition mode PFC controller

Figure 13. Schematic of the sepic converter



4.2 Bench results

The diagrams in this section summarize the results of certain bench evaluations. They also show waveforms under different load and line conditions.

Figure 14 illustrates the measured efficiency for different loads (65 W, 38 W and 22 W of output power) versus the input ac voltage.

Figure 15 demonstrates the MOSFET drain voltage (Ch4), the output voltage (Ch3) and the input voltage.

The quantities that indicate the quality of the input current as power factor, THD (Total Harmonic Distortion) and crest factor, where measured at full load and for different input voltages. They are reported in *Table 3*.

Figure 16 to *Figure 19* show the currents flowing in the two inductors (Ch1: L1 current; Ch2: L2 current) for different load conditions. Letting the input voltage of the converter (the rectified main) be a perfect rectified sinusoid, it may be used as a reference and is shown as Ch4 in the above figures.

Figure 20 illustrates the input current (Ch1) measured before the input bridge diodes. The voltage at the input of the bridge diodes (Ch4) is also shown as a reference.

Figure 20 is input current at full load (65 W) with 230 V_{ac} as input voltage. *Figure 21* is input current at half load (32 W) with 230 V_{ac} as input voltage.

Table 3. Input current quality measurements

P _{out} = 65 W			
Input voltage (V _{RMS})	PFC	THD %	Crest factor
175	0.992	10.3	1.35
220	0.986	12.3	1.36
230	0.984	12.6	1.37
265	0.975	14.2	1.46

Figure 14. Efficiency chart

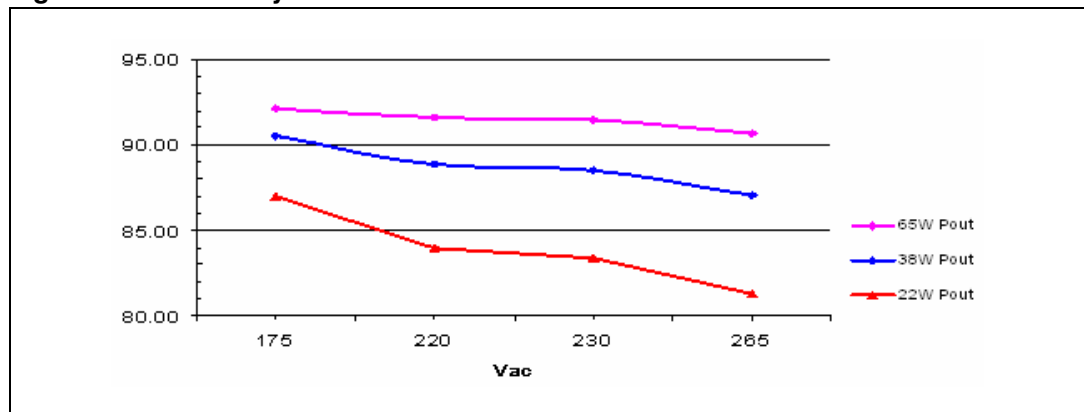
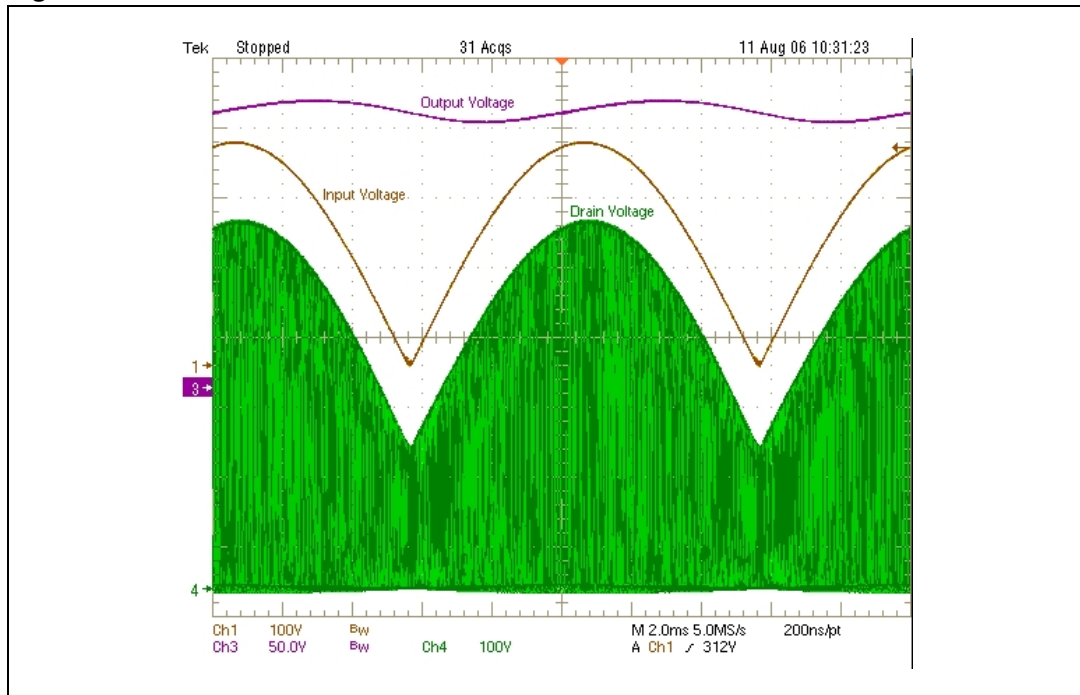


Figure 15. Main waveform of the circuit



1. Test conditions include $P_{out} = 65\text{ W}$ and $V_{in} = 230\text{ V}_{ACRMS}$.

Figure 16. Current of the inductors over one line cycle: $V_{in} = 230 V_{ACRMS}$, $P_{out} = 65 W$

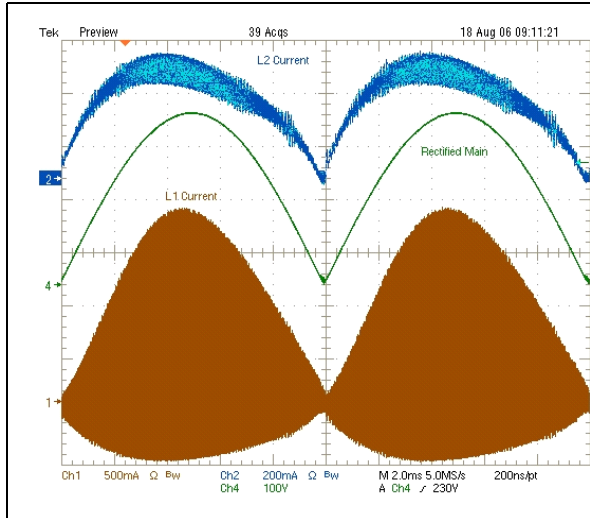


Figure 17. Current of the inductors over switching cycles: $V_{in} = 230 V_{ACRMS}$, $P_{out} = 65 W$

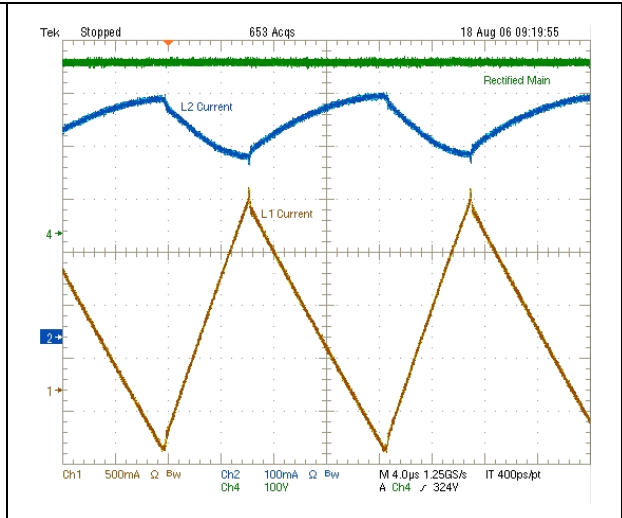


Figure 18. Current of the inductors over one line cycle: $V_{in} = 230 V_{ACRMS}$, $P_{out} = 65 W$

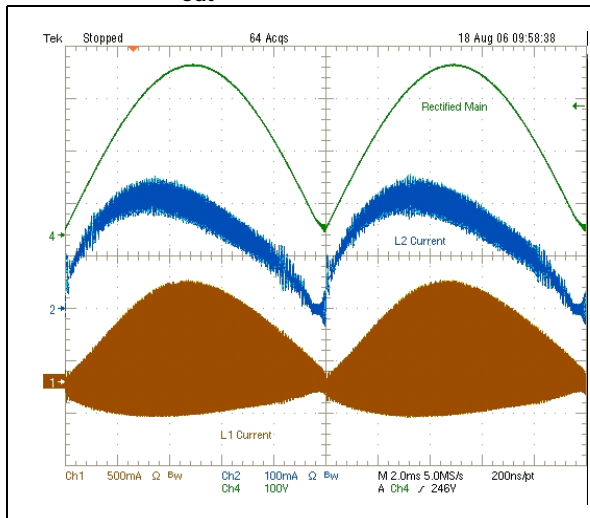


Figure 19. Currents of the inductors over switching cycles: $V_{in} = 230 V_{ACRMS}$, $P_{out} = 65 W$

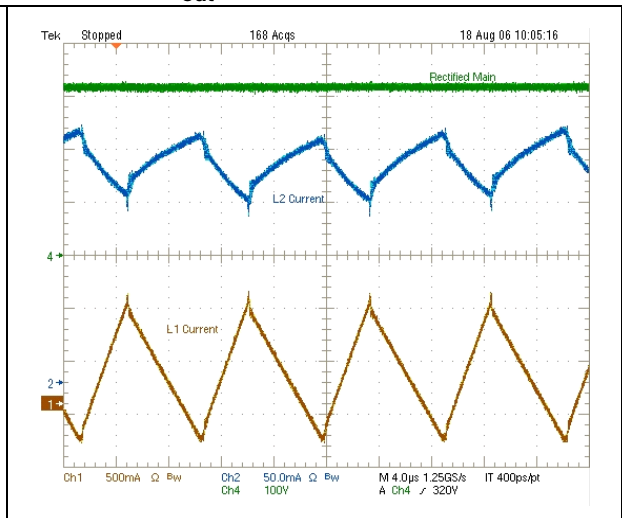


Figure 20. Input current: 230 V_{ac} input, 65 W output

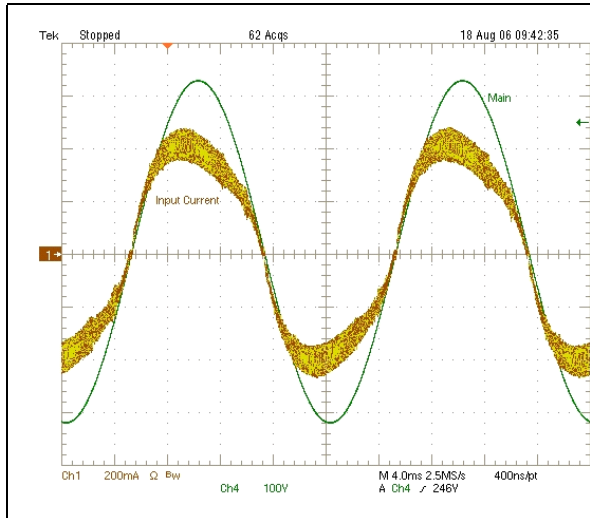
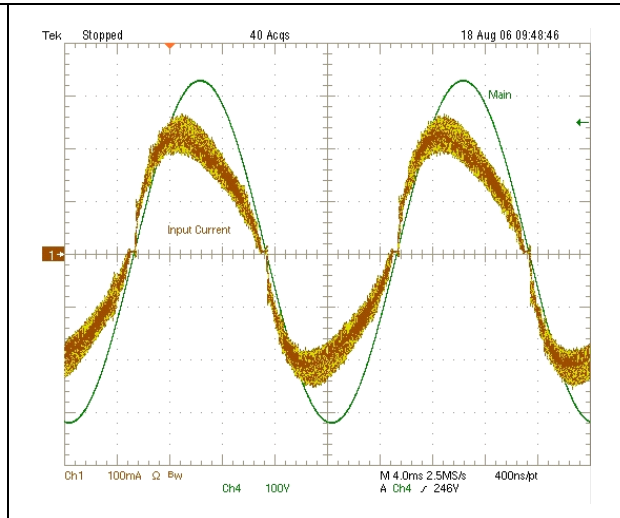


Figure 21. Input current: 230 V_{ac} input, 32 W output



5 Revision history

Table 4. Revision history

Date	Revision	Changes
05-Mar-2007	1	First issue

Please Read Carefully:

Information in this document is provided solely in connection with ST products. STMicroelectronics NV and its subsidiaries ("ST") reserve the right to make changes, corrections, modifications or improvements, to this document, and the products and services described herein at any time, without notice.

All ST products are sold pursuant to ST's terms and conditions of sale.

Purchasers are solely responsible for the choice, selection and use of the ST products and services described herein, and ST assumes no liability whatsoever relating to the choice, selection or use of the ST products and services described herein.

No license, express or implied, by estoppel or otherwise, to any intellectual property rights is granted under this document. If any part of this document refers to any third party products or services it shall not be deemed a license grant by ST for the use of such third party products or services, or any intellectual property contained therein or considered as a warranty covering the use in any manner whatsoever of such third party products or services or any intellectual property contained therein.

UNLESS OTHERWISE SET FORTH IN ST'S TERMS AND CONDITIONS OF SALE ST DISCLAIMS ANY EXPRESS OR IMPLIED WARRANTY WITH RESPECT TO THE USE AND/OR SALE OF ST PRODUCTS INCLUDING WITHOUT LIMITATION IMPLIED WARRANTIES OF MERCHANTABILITY, FITNESS FOR A PARTICULAR PURPOSE (AND THEIR EQUIVALENTS UNDER THE LAWS OF ANY JURISDICTION), OR INFRINGEMENT OF ANY PATENT, COPYRIGHT OR OTHER INTELLECTUAL PROPERTY RIGHT.

UNLESS EXPRESSLY APPROVED IN WRITING BY AN AUTHORIZED ST REPRESENTATIVE, ST PRODUCTS ARE NOT RECOMMENDED, AUTHORIZED OR WARRANTED FOR USE IN MILITARY, AIR CRAFT, SPACE, LIFE SAVING, OR LIFE SUSTAINING APPLICATIONS, NOR IN PRODUCTS OR SYSTEMS WHERE FAILURE OR MALFUNCTION MAY RESULT IN PERSONAL INJURY, DEATH, OR SEVERE PROPERTY OR ENVIRONMENTAL DAMAGE. ST PRODUCTS WHICH ARE NOT SPECIFIED AS "AUTOMOTIVE GRADE" MAY ONLY BE USED IN AUTOMOTIVE APPLICATIONS AT USER'S OWN RISK.

Resale of ST products with provisions different from the statements and/or technical features set forth in this document shall immediately void any warranty granted by ST for the ST product or service described herein and shall not create or extend in any manner whatsoever, any liability of ST.

ST and the ST logo are trademarks or registered trademarks of ST in various countries.

Information in this document supersedes and replaces all information previously supplied.

The ST logo is a registered trademark of STMicroelectronics. All other names are the property of their respective owners.

© 2007 STMicroelectronics - All rights reserved

STMicroelectronics group of companies

Australia - Belgium - Brazil - Canada - China - Czech Republic - Finland - France - Germany - Hong Kong - India - Israel - Italy - Japan - Malaysia - Malta - Morocco - Singapore - Spain - Sweden - Switzerland - United Kingdom - United States of America

www.st.com

